Fatigue Crack Propagation Characteristics of Welded Joints in a 444 Stainless Steel

Masayuki AKITA[1)], Masaki NAKAJIMA[2)], Keiro TOKAJI[1)] & Toshihiro SHIMIZU[2)]

[1]Faculty of Engineering, Gifu University, Gifu 500-1193, Japan

[2]Department of Mechanical Engineering, Toyota National College of Technology, Aichi 471-8525, Japan

ABSTRACT

This paper describes the fatigue crack propagation (FCP) behavior for large cracks of a ferritic stainless steel welded joints. FCP experiments were performed using electro-hydraulic fatigue testing machine in laboratory air and in 3%NaCl aqueous solution. Three types of welded CT specimens, the specimens in which the starter notch was introduced perpendicular to the weld line, within HAZ (Heat Affected Zone) and within the weld metal, were evaluated. In laboratory air, when the crack propagated normal to the weld line, FCP behavior was rather complicated and FCP rates decreased temporarily as it reached HAZ and then increased with crack propagation within HAZ. When the crack propagated within HAZ and the weld metal parallel to the weld line, FCP rates were significantly lower than those of the base metal in the entire ΔK region. After allowing for crack closure, however, the FCP data of all the welded specimens became similar and agreed with those of the base metal. In 3%NaCl aqueous solution, the FCP rates of all the welded specimens were still enhanced at high ΔK_{eff} regime, where some intergranular fracture and quasi-cleavage fracture were seen, which was due to an environmental effect.

1 INTRODUCTION

Ferritic stainless steels posses an excellent resistance to stress corrosion cracking (SCC), while they have poor toughness and as-welded ductility. In recent years, new ferritic stainless steels with extremely reduced (C+N) content have been developed, in which toughness and weldability are significantly improved[1), 2)].

Welded joints are widely used in machine components and structures, thus evaluation on the fatigue properties of welded joints is particularly important to ensure their safety and reliability. However, there have been very limited studies on fatigue behavior in not only ferritic stainless steels themselves[3)], but also welded joints. In addition, since stainless steels are generally used in corrosive environments, it is also necessary to understand their fatigue behavior in such environments.

In the present study, fatigue crack propagation (FCP) behavior for large cracks was studied on welded joints of a ferritic stainless steel, type 444. The obtained results were discussed on the basis of residual stress, crack closure behavior and fracture surface analysis.

2 EXPERIMENTAL PROCEDURES

2.1 Material and specimens

The base metal used in this study is a ferritic stainless steel, type 444 (18Cr-2Mo) whose chemical composition (mass %) is C: 0.004, Si: 0.06, Mn: 0.1, P: 0.024, S: 0.006, Ni: 0.11, Nb: 0.17, Cr: 18.72, Mo: 1.81, V: 0.06, N: 0.068. The mechanical properties for two directions parallel and perpendicular to the rolling direction (L and T directions) are shown in Table 1. The proof stress and tensile strength in the T direction are slightly higher than those in the L direction.

Table 1 Mechanical properties of the base metal.

Direction	0.2%proof stress $\sigma_{0.2}$ (MPa)	Tensile strength σ_B (MPa)	Breaking strength on final area σ_T (MPa)	Elongation φ (%)	Reduction of area ψ (%)
L	293	445	1480	34	83
T	310	460	1352	31	81

Three types of welded CT specimens, i.e. the specimen with weld line normal to the FCP direction (N-specimen), the specimens with FCP within HAZ (H-specimen) and within the weld metal (W-specimen) respectively, were evaluated. The welding direction was parallel to the T direction, thus the FCP direction was the L direction in N-specimens, while the T direction in H-specimens and W-specimens.

2.2 Welding condition

Welding was performed by the tungsten-inert gas welding method (TIG) with a root opening of 1.6mm, an X-shape groove, the voltage of 20V and 3 welding passes on both sides. The filler metal was a 309L austenitic stainless steel.

Before FCP experiment, microstructure and hardness around the weld zone were evaluated. As a result, the average grain size was 56μm and 123μm for the base metal and HAZ, respectively and Vickers hardness was 162*HV*, 172*HV* and 194*HV* for the base metal, HAZ and the weld metal, respectively.

2.3 Experimental procedures

FCP tests were performed at a stress ratio of 0.05 using a 19.6kN capacity electro-hydraulic fatigue testing machine operating at a frequency of 1Hz. Test environments employed were laboratory air and 3%NaCl aqueous solution. Crack closure was measured by an unloading elastic compliance method. After experiment, fracture surfaces were examined using a scanning electron microscope (SEM).

3 RESULTS

3.1 Residual stress distribution

Residual stress for the welded specimens was measured by the X-ray diffraction method. Figure 1 shows the distribution of residual stress normal to the FCP direction in the N-specimens. Residual stresses are approximately -110~-480MPa at the top surface (the side of the first pass), while are -100~-500MPa at the bottom surface (the opposite side of the second pass). Compressive residual stresses decrease as the distance from the notch root increases toward the weld zone. From this measured residual stress

distribution, it is believed that large tensile residual stress would generate in the welded metal.

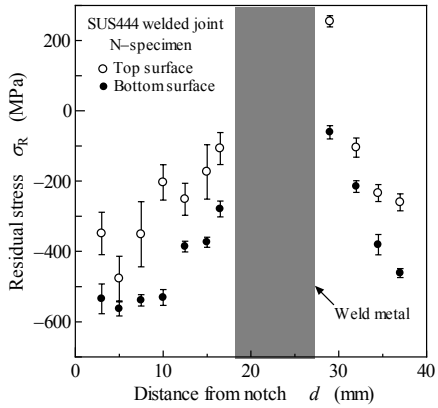

Fig.1 Distribution of residual stress normal to the FCP direction in N-specimens.

3.2 FCP behavior of welded joints

The FCP behavior for the N-specimens, H-specimens and W-specimens is shown in Fig.2. For comparison, the FCP behavior for the base metal is also included in those figures.

3.2.1 N-specimen (Fig.2(a))

In laboratory air, the FCP rates are almost the same as those for the base metal in low ΔK region. With increasing crack growth, fluctuation of FCP rate becomes remarkable and the FCP rates decrease temporarily around ΔK=20MPam$^{1/2}$, then increase and approach those for the base metal. Such a complicated FCP behavior appears to be due to residual stress and hardness changes induced by welding. In 3%NaCl solution, the FCP rates are considerably lower than those for the base metal and fluctuation of FCP rate is not seen.

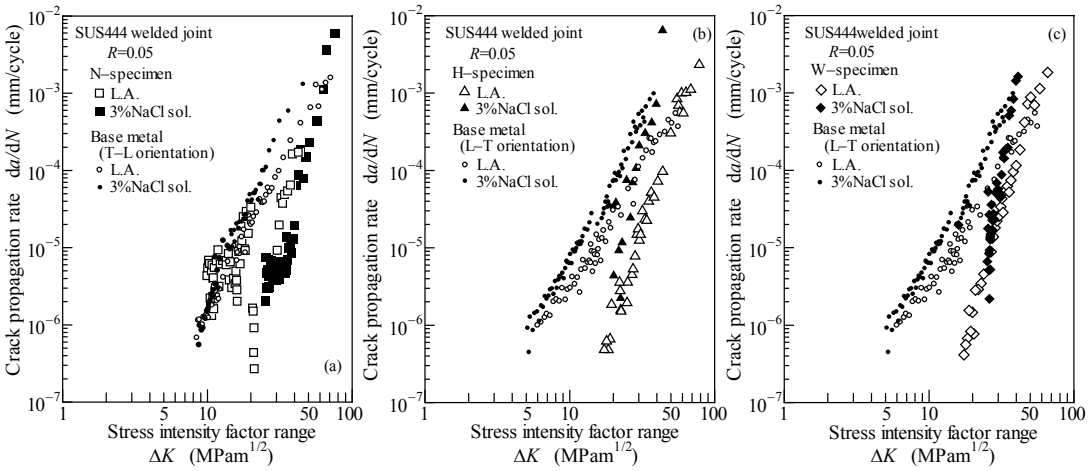

Fig.2 FCP behavior of welded joints: (a) N-specimen, (b) H-specimen, (c) W-specimen.

3.2.2 H-specimen and W-specimen (Fig.2(b) and Fig.2(c))

In laboratory air, the FCP rates of H-specimens and W-specimens are lower than those for the base metal in the entire ΔK region and with increasing ΔK gradually approach and then coincide with the FCP rates for the base metal at high ΔK region, indicating higher FCP resistance of HAZ and the weld metal than the base metal.

In 3%NaCl solution, the FCP rates are faster than those in laboratory air, which becomes more pronounced with increasing ΔK. When compared with the data for the base metal, the FCP rates are lower in the entire ΔK region, particularly remarkable at low ΔK region.

4 DISCUSSION

4.1. FCP behavior of welded specimens in laboratory air

In laboratory, the N-specimens air showed remarkable fluctuation of FCP rate with increasing crack length and a large decrease in FCP rate around ΔK=20MPam$^{1/2}$. It has been well known that residual stress plays an important role in the FCP behavior of welded joints. Figure 3 represents the FCP behavior and residual stress change in the N-specimens as a function of crack length in both environments. As described above, the FCP behavior is rather complicated in laboratory air, and it is worth noting that the FCP rate is significantly decreased just before the crack reaches HAZ. On the other hand, compressive residual stresses decrease monotonously with increasing crack length. Therefore, this residual stress change does not correspond to the remarkable decrease in FCP rate just before reaching HAZ. The similar results have been reported in laser welded butt joints, which seems to be due to a sudden hardness change at the boundary between the base metal and HAZ[4]. In spite of the existence of compressive residual stress, the FCP rates for the welded specimens were almost the same as those for the base metal at low ΔK region, this is because the compressive residual stress of -200~-400MPa was detected in the base metal, which is equivalent to the compressive residual stresses in the welded specimens.

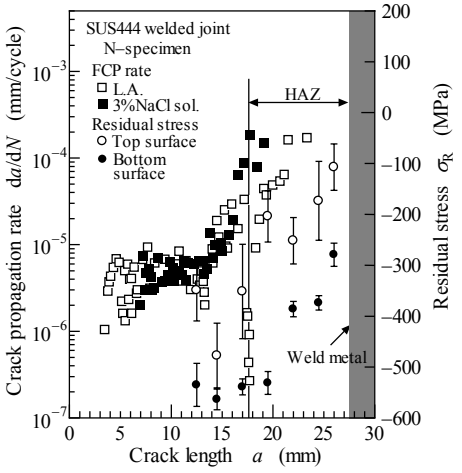

Fig.3 Relationship between FCP rate and residual stress distribution in N-specimens.

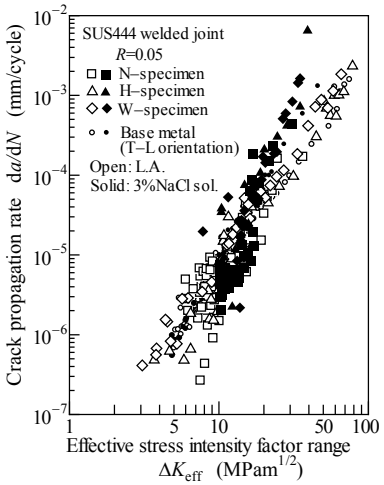

Fig.4 FCP behavior characterized in terms of effective stress intensity factor range in welded specimens.

As seen in Fig.3, the results in 3%NaCl solution did not show complicated FCP behavior as seen in

laboratory air. This is due to the larger ΔK employed in the experiment, thus the effect of HAZ becomes relatively small.

In the H-specimens and W-specimens, the crack propagates within HAZ and the weld metal, respectively. Compressive residual stress of nearly -300MPa and tensile residual stress of 100MPa are present at the top and bottom surfaces in HAZ, respectively. Residual stress in the weld metal could not be measured, but it is assumed that the similar residual stresses would be present. Although it is not easy to understand the effect of residual stress in such a case, i.e. compressive on one side and tensile on the opposite side, it seems that the FCP behavior is affected by compressive residual stress rather than tensile residual stress, because the absolute value of the former is significantly larger than that of the latter. In addition to residual stress, deflection of crack path was much more remarkable in HAZ and the weld metal due to grain growth and solidifying microstructure, respectively, which also contributes higher FCP resistance in HAZ and the weld metal than the base metal.

4.2. FCP behavior after allowing for crack closure

FCP behavior characterized in terms of the effective stress intensity factor range, ΔK_{eff}, is shown in Fig.4. The da/dN-ΔK_{eff} relationships for all of the welded specimens are almost identical to that of the base metal. Therefore, the differences observed in the da/dN-ΔK relationships among the welded specimens and between the welded specimens and the base metal are attributed to crack closure that is induced by residual stress and fracture surface roughness.

In 3%NaCl solution, the da/dN-ΔK_{eff} relationships in all of the welded specimens are nearly the same, thus the difference observed in the da/dN-ΔK relationships among the welded specimens is also attributed to crack closure. However, when compared with the da/dN-ΔK_{eff} relationships in laboratory air, the FCP rates in 3%NaCl solution is significantly faster in the region of ΔK_{eff}>15~20MPam$^{1/2}$, indicating that a pure environmental effect exists in that region.

4.3 Effect of corrosive environment on FCP behavior

As indicated above, the FCP rates of the welded specimens were still faster at high ΔK_{eff} region in 3%NaCl solution. The fracture surface was examined using SEM and the micrographs are shown in Fig.5. The fracture surfaces in low ΔK region were ductile transgranular, which is similar to those in laboratory air. As seen in Fig.5, however, some intergranular fracture or quasi-cleavage fracture can be seen in the welded specimens. This clearly indicates that different fracture mechanisms from in laboratory air operated in 3%NaCl solution.

SCC and hydrogen embrittlement are believed to be the causes of brittle fracture in 3%NaCl solution, but the effect of SCC would be negligible, because it has been indicated that ferritic stainless steels have very low susceptibility to SCC in a highly concentrated chloride solution[5]. In reality, SCC tests have been performed using CT specimens of the present 444 steel in 3%NaCl solution, but SCC did not take place. Therefore, it is believed that hydrogen embrittlement of ferritic phase[6] would be responsible for the accelerated FCP in 3%NaCl solution. In addition, it has been indicated that HAZ becomes sensitive to intergranular fracture in ferritic stainless steel weldments[7].

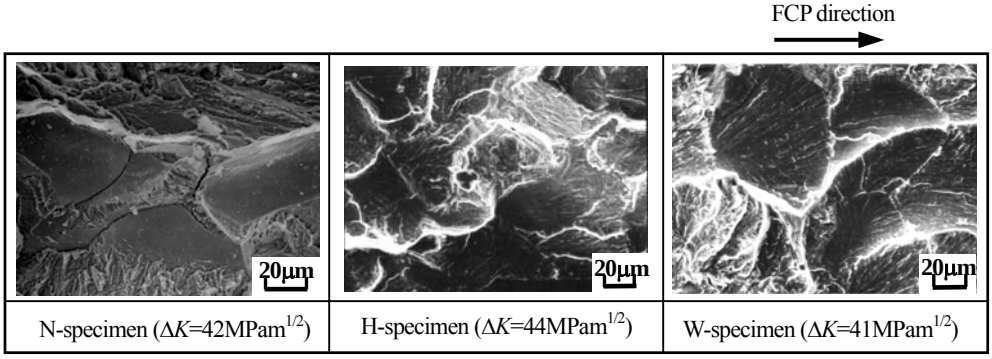

Fig.5 Fracture surface appearance of welded specimens in the FCP regime enhanced by 3%NaCl solution.

5 CONCLUSIONS

(1) In laboratory air, the welded specimens in which the crack propagated perpendicular to the weld line showed complicated FCP behavior with frequent fluctuations in FCP rate. When the crack reached HAZ, the FCP rates were significantly decreased and then monotonously increased. When the crack propagated within HAZ and the weld metal parallel to the weld line, the FCP rates for both specimens were almost identical and lower than those for the base metal in the entire ΔK region.

(2) In 3%NaCl solution, the FCP rates of all the welded specimens were accelerated compared with those in laboratory air, being more pronounced with increasing ΔK.

(3) In laboratory air, after allowing for crack closure, the all welded specimens showed nearly the same FCP behavior, indicating that the observed differences in the FCP rate characterized in terms of ΔK were attributed to crack closure.

(4) After allowing for crack closure, the FCP rates in 3%NaCl solution were still faster at high ΔK_{eff} than those in laboratory air, where extensive intergranular fracture and quasi-cleavage were seen.

REFFERENCES

1) T.Nakazawa, S.Suzuki, T.Sunami and Y.Sogo, Application of High-Purity Ferritic Stainless Steel Plates to Welded Structures, *ASTM STP*, **706** (1980), 99.

2) J.D.Redmond, Toughness of 18Cr-2Mo Stainless Steel, *ASTM STP*, **706** (1980), 123.

3) A.Celik and A.Alsaran, Mechanical and Structural Properties of Similar and Dissimilar Steel Joints, *Mater. Characterization*, **43**(1999), 311.

4) A.Minagi and K.Tokaji , Fatigue Crack Propagation of Laser Welded Butt Joints, Tetsu-to-Hagane, **86** (2000), 51. (In Japanese).

5) M.Kowaka, The Corrosion Behavior of Ferritic Stainless Steels, *J. Soc. Mater. Sci., Jpn.*, **23** (1974), 924 (In Japanese).

6) K.Komai and K.Irifune, Corrosion Fatigue Crack Growth Behavior of Dual-Phase Stainless Steel in Synthetic Sea Water, *J. Soc. Mater. Sci., Jpn.*, **36** (1987), 1104(In Japanese).